NC-SIMC: Neuro-Controller Simple Internal Model Control

Erbet Almeida Costa * **Sigurd Skogestad** *
Idelfonso dos Reis Nogueira *

* *Department of Chemical Engineering, Norwegian University of Science and Technology, Gløshaugen, Trondeim, Norway (e-mail: erbet.a.costa@ntnu.no, sigurd.skogestad@ntnu.no, idelfonso.b.d.r.nogueira@ntnu.no).*

Abstract: This study introduces a novel Neuro-Controller Simple Internal Model Control (NC-SIMC) paradigm. Our primary goal is to develop a neural network architecture that integrates the logical principles of Proportional-Integral-Derivative (PID) controller design, as outlined by the SIMC rules, into a model capable of generating control actions without the necessity for training with closed-loop data. This is achieved by employing the Simple Internal Model Control framework to effectively train the adapted neural network structure. We present a machine-learning approach that combines a specialized inductive bias node by using a custom new layer inside the neutral net structure to address this goal. Hence, it bridges traditional control theory and machine learning. A key innovation of our NC-SIMC approach is its ability to learn and internally formulate a control structure and parameters. This enables it to establish suitable control actions based on the system's state, setpoint, and feedback without relying on a fixed control structure. Our paper demonstrates the efficacy of NC-SIMC in stabilizing control actions and its adaptability across various operating conditions without requiring retuning. This performance is shown to be favorably comparable to traditional SIMC rules. We conclude by discussing the potential for future improvements in dynamic performance and the integration of constraints directly into the inductive bias layer, opening new avenues for advanced control system design. The main advantage of our strategy is that no closed-loop data is needed to identify the NC-SIMC PID controller. Instead, the model learns from the SIMC rules.

Keywords: PID control design based on artificial intelligence methods; PID tuning and automatic tuning methodologies; Adaptive and robust PID control.

1. INTRODUCTION

The theoretical basis of our Neuro-Controller Simple Internal Model Control (NC-SIMC) development is grounded in the established principles of traditional PID controller design. PIDs have a well-established body of literature and are applied across all segments of dynamic system control. Over the years, various methods for formulation and tuning such controllers have been proposed, including Ziegler and Nichols (1942), the Internal Model Control (IMC) presented in Rivera et al. (1986); Garcia and Morari (1982), and the SIMC approach by Skogestad (2003). Traditionally, PID controller tuning focuses on the system's open-loop behavior, followed by its application in a closed-loop setting. This method involves identifying key system parameters and determining appropriate tuning adjustments to enhance robustness and performance to meet specific scenarios. Given the simplicity of PID controllers, the main challenge in implementation is the selection of tuning parameters, which is why the cited works are so significant and shed light on the field of controller tuning.

The advent of artificial intelligence has led to a growing interest in AI-powered PID controllers, as evidenced by their increasing prevalence in recent literature. These AI-based solutions, however, typically necessitate training with open-loop data before being deployed in a closed-loop system (Zribi et al., 2015). This requirement represents a significant limitation of the AI approach to PID control. The training process demands extensive data collection and analysis, which can be time-consuming and may only sometimes accurately represent a system's full range of operational scenarios. On the other hand, several works have proposed different structures of neural nets to tune an existing PID structure Zribi et al. (2015); Badr (1997); Hernández-Alvarado et al. (2016); Xu (2022); de Moura et al. (2020).

Furthermore, many of these AI strategies are often presented as alternatives to traditional control theory rather than as complementary approaches. This perspective overlooks the rich, established knowledge base within traditional control theory. By positioning AI-based methods as replacements rather than as enhancements or extensions, there is a risk of missing valuable insights and principles that traditional control theory offers. A more integrated approach, which combines AI's adaptability and learning capabilities with the foundational principles of traditional PID control, could lead to more robust and effective control systems. Such an approach would leverage the

strengths of both AI and traditional methods, potentially overcoming the limitations of each when used in isolation.

In this context, the primary contribution of our work in developing the (NC-SIMC, Neuro-Controller Simple Internal Model Control, or Nogueira-Costa- Skogestad Internal Model Control) lies in its integration of artificial intelligence with traditional PID control principles by inductive bias. Without needing an extensive database, the proposed neural structure learns from the well-established SIMC rules and uses a novel internal PID layer to compute the control actions. By blending AI's adaptability and advanced learning capabilities with the robustness and reliability of traditional PID control methods, the NC-SIMC offers a more versatile and efficient solution for modern control systems. The inductive bias layer plays a crucial role, allowing the control action values to be obtained by the network based on a customized neuron that contains a PID function as an activation function. Hence, the control actions are calculated by a specifically constructed output layer, making the values of the closed-loop control actions unnecessary in the training step of the methodology.

The paper's subsequent sections are as follows: Section 2 presents the proposed methodology. Section 3 discusses the test results for a polymerization reactor, and Section 4 concludes the paper.

2. METHODOLOGY

The initial step in the process is the open-loop excitation of the system at various operating points. The excitation's amplitude and frequency are determined using a Latin Hypercube Sampling algorithm. Using the open-loop response values of the system, identification is performed at the sampled operating points to approximate the system to a first or second-order plus time delay transfer function as:

$$g(s) = \frac{k}{(\tau_1 s + 1)(\tau_2 s + 1)} e^{-\theta s} \tag{1}$$

The SIMC tuning for the series PID rules proposed by Skogestad (2003) with good robustness are:

$$K_c = \frac{0.5}{k} \frac{\tau_1}{\theta} \tag{2}$$

$$\tau_I = min\{\tau_1, 8\theta\} \tag{3}$$

$$\tau_D = \tau_2. \tag{4}$$

Additionally, when a first-order plus time delay approximates the system, the time constant $\tau_2 = 0$, then, $\tau_D = 0$, the other rules are the same (Skogestad, 2003). Therefore, in this paper, only PI controllers are evaluated.

With the rules, it is possible to build the training, validation, and test sets for building the NC-SIMC controller. To do so, apply Equations (2)-(4) rules to each stationary state identified through the LHS inserted into the system.

Once the tuning values for the different operating points have been identified, the construction of the NC-SIMC controller proceeds. In this methodology phase, the neural network shown in Figure 1 is trained to provide the control action of a PI controller based on the system's current state. Also, the learning function is defined as:

$$\text{MSE} = \frac{1}{n} \sum_{i=1}^{n} (K_{ci} - \hat{K}_{ci})^2 + \frac{1}{n} \sum_{i=1}^{n} (\tau_{Ii} - \hat{\tau}_{Ii})^2$$

in which K_{ci} and τ_{Ii} are the tuning obtained by the SIMC rules and $\hat{K}_{ci}$ and $\hat{\tau}_{Ii}$ are the values predicted by the NC-SIMC.

In the final layer of our model's architecture, we introduce a specialized component known as the PI-reinforced node. This node functions as an inductive bias element and is a customized neuron. Its activation function is designed to mimic that of a PI controller, effectively integrating the principles of Proportional-Integral control. This node receives a bias from two system components: the error and integral. This design choice ensures that the node's response is closely aligned with the dynamic behavior of a PI controller, thereby enhancing the model's ability to manage system errors in a manner akin to traditional control systems but with the added adaptability and learning capabilities of a neural network.

The network structure weights and biases presented in Figure 1 are obtained through offline training that does not depend on the closed-loop operation. In this way, the network is trained to provide tuning for the controller. This last node includes a bias composed of the current error between the setpoint and the measured variable plus the integral of the error.

The network's hyperparameters, type and number of layers, neurons, and activation functions, among others, can be defined through an optimization algorithm such as the one proposed by Li et al. (2016). These algorithms search for an optimized network structure from a search region. Using such algorithms significantly reduces the need for testing to verify whether or not the network has an adequate structure and facilitates network construction.

When the NC-SIMC controller is operating, it considers the current values of the measured variables and inputs and adapts the control action accordingly. This makes NC-SIMC adaptive and suitable for working over an extensive operating range without retuning the PI control.

3. RESULTS

This study focuses on a styrene polymerization reactor, crucial in polymer production, and utilizes the mathematical models proposed by Hidalgo and Brosilow (1990) and Alvarez and Odloak (2012). The process begins with initiator decomposition and radical formation, leading to live polymer chain generation. Chain growth occurs by adding monomers until the radicals deactivate into dead polymer chains. The operational model of the reactor excludes monomer and solvent chain transfers, emphasizing monomer consumption and the short-lived nature of polymer radicals. Operational temperatures negate thermal monomer initiation concerns. Additionally, the model considers the chain termination rate and deems the heat from initiation and termination negligible compared to

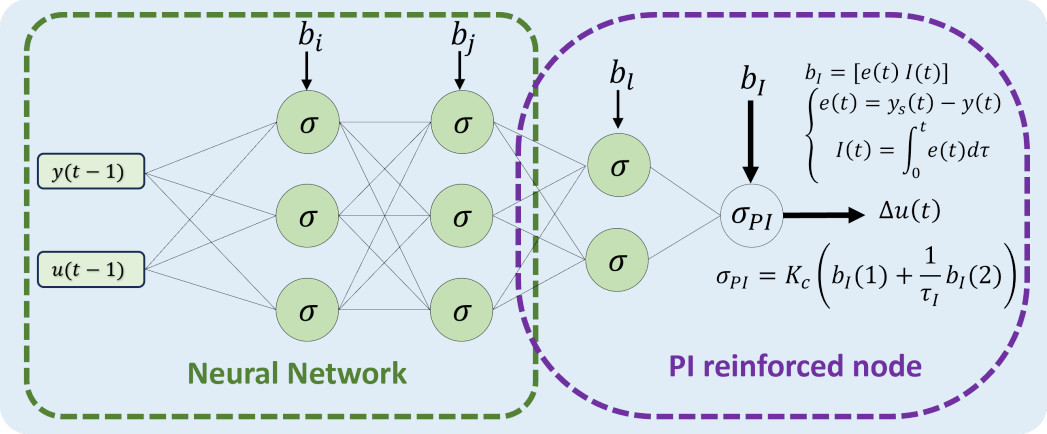

Fig. 1. Methodology chart.

the heat of polymerization. The equations are outlined by Alvarez and Odloak (2012) as:

$$\frac{d[M]}{dt} = \frac{Q_m[M_f] - Q_t[M]}{V} - k_p[M][P], \tag{5}$$

$$\frac{d[I]}{dt} = \frac{Q_i[I_f] - Q_t[I]}{V} - k_d[I], \tag{6}$$

$$\frac{dD_0}{dt} = 0.5k_t[P]^2 - \frac{Q_t D_0}{V}, \tag{7}$$

$$\frac{dD_1}{dt} = M_m k_p[M][P] - \frac{Q_t D_1}{V}, \tag{8}$$

$$\frac{dD_2}{dt} = 5M_m k_p[M][P] + M_m\frac{k_p^2}{k_t}[M]^2 - \frac{Q_t D_2}{V}, \tag{9}$$

$$\frac{dT}{dt} = \frac{Q_i[T_f - T]}{V} + \frac{-\Delta H_r}{\rho C_p}k_p[M][P] - \frac{hA}{\rho C_p V}(T - T_c), \tag{10}$$

$$\frac{dT_c}{dt} = \frac{Q_c(T_{cf} - T_c)}{V_c} + \frac{hA}{\rho C_p V}(T - T_c), \tag{11}$$

$$k_j = A_j exp\left(\frac{-E_j}{T}\right),\ j = d,\ p,\ t, \tag{12}$$

$$[P] = \left[\frac{2f_i k_d[I]}{k_t}\right]^{0.5}, \tag{13}$$

$$Q_t = Q_i + Q_s + Q_m, \tag{14}$$

$$PD = M_m\frac{D_2 D_0}{D_1^2}, \tag{15}$$

The differential equation set encapsulates the dynamic behavior of monomer, initiator, dead-polymer chains, and live-polymer chains in a styrene polymerization reactor. Each differential equation delineates the temporal concentration change of these entities, incorporating reaction kinetics, feed rates, and volumetric variations. The rate constants for propagation, initiation, termination via combination, and termination through disproportionation are symbolized by k_p, k_i, k_t, and k_{td} respectively. Concentrations of monomer, initiator, and live-polymer chains with n units, and reactor temperature are represented by $[M]$, $[I]$, $[P_n]$, and $[T]$. The flow rates for the reactor's output and input are given by F and F_{in} while M_f, I_f, and T_f indicate the monomer, initiator, and temperature concentrations at the input, respectively. V denotes the reactor's volume.

In this system, two variables are used for control purposes. The first is the reactor temperature (T) (Equation 10), and the second is the average molecular weight of the polymer produced given by Alvarez and Odloak (2012):

$$\bar{M}_w = M_m\frac{D_2}{D_1}. \tag{16}$$

However, the average molecular weight may not be measurable, so Odloak suggests that an alternative approach is to control the polymer's viscosity:

$$\eta = 0.0012(\bar{M}_w)^{0.71}. \tag{17}$$

These variables are directly linked to the quality of the polymer produced, and meeting the necessary specifications can be achieved through their control. The initiator flow rates and the cooling jacket fluid flow rate are selected as manipulated variables. In contrast, the flow rates of monomer and solvent are considered unknown disturbances by the control loops. Viscosity and temperature control can thus be achieved by pairing the viscosity and initiator flow rate ($\eta \times Qi$) and the reactor temperature with the cooling jacket feed flow rate ($T \times Qc$).

A first-order transfer function model was used to approximate the system response. This implies that the derivative action is not used. Only the proportional and integral actions are to generate the training, validation, and test sets to build the NC-SIMC controller for the reactor described by Equations (5)-(17). Also, a set of random signals was created using a Latin Hypercube Sampler to perform the open-loop tests. The operational region was defined based on the values presented in Table 2, allowing for a 50 % variation in the input variables either way. These signals were simulated using Equations (5)-(17), and the response was used to identify a transfer function for each of the steady states reached. With the identified parameters in hand, the SIMC rules were applied to obtain the tuning parameters displayed in Figure 2. In Figure 2, histograms show the distributions of each parameter, whereas the solid line indicates the respective nominal value for the parameter. This nominal value is obtained in the steady state reached with the input values from Table 2. Additionally, these values are used to tune the SIMC controller and serve as a benchmark for evaluating the NC-SIMC controller in the subsequent discussion.

Table 1. Model parameters and initial conditions (Alvarez and Odloak, 2012).

Nominal Process Parameters	Value
Frequency factor for initiator decomposition, $A_d(h^{-1})$	2.142×10^{17}
Activation energy for initiator decomposition, $E_d(K)$	14897
Frequency factor for propagation reaction, $A_p(L \cdot mol^{-1} \cdot h^{-1}$	3.81×10^{10}
Activation temperature for propagation reaction, $E_p(K)$	3557
Frequency factor for termination reaction, $A_t(Lmol^{-1}h^{-1})$	4.50×10^{12}
Activation temperature for termination reaction, $E_t(K)$	843
Initiator efficiency, f_i	0.6
Heat of polymerization, $-\Delta H_r(J \cdot mol^{-1})$	6.99×10^4
Overall heat transfer coefficient, $hA(J \cdot K^{-1} \cdot L^{-1})$	1.05×10^6
Mean heat capacity of reactor fluid, $\rho C_p(JK^{-1}L^{-1})$	1506
Heat capacity of cooling jacket fluid, $\rho_c C_p c(JK^{-1}L^{-1})$	4043
Molecular weight of the monomer, $M_m(g \cdot mol^{-1})$	104.14
Initial conditions	**Value**
Reactor volume, $V(L)$	3000
Volume of cooling jacket fluid, $Vc(L)$	3312.4
Concentration of initiator in feed, $I_f(mol \cdot L^{-1})$	0.5888
Concentration of monomer in feed, $M_f(mol \cdot L^{-1})$	8.6981
Temperature of reactor feed, $T_f(K)$	330
Inlet temperature of cooling jacket fluid, $Tcf(K)$	295

Table 2. Steady-state inputs conditions and region of sampling for the LHS algorithm.

Variable	Steady-state	Minimum	Maximum
Initiator flow rate, $Q_i(L \cdot h^{-1})$	108	91.8	124.2
Solvent flow rate, $Q_s(L \cdot h^{-1})$	3312.4	2815.5	3809.26
Monomer flow rate, $Q_m(L \cdot h^{-1})$	0.5888	0.5005	0.6771
Cooling jacket fluid flow rate, $Q_c(L \cdot h^{-1})$	8.6981	7.3934	10.0028

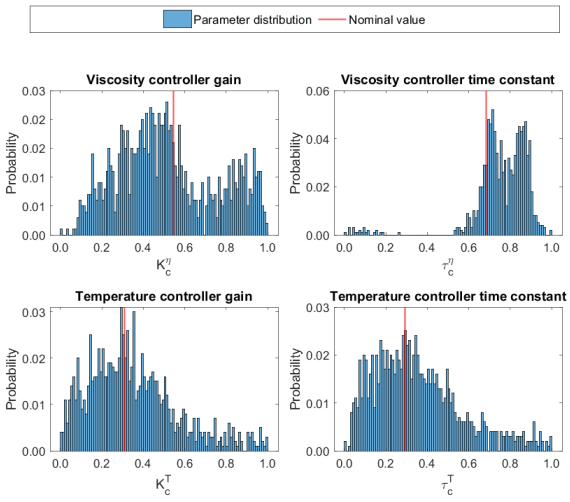

Fig. 2. SIMC data for training, test, and validation datasets. The datasets were selected randomly with the following proportions: Train 70%, Validation 15%, and Test 15%.

The first scenario for comparing the controllers is shown in Figure 3. The controllers were directly tested on the nonlinear system from Equations (5)-(17). In the scenario of Figure 3, the SIMC and NC-SIMC controllers are tested against setpoint changes, disturbances at the inputs, and unmeasured in the presence of measurement noise. At the 100-hour mark, the first setpoint change occurs in temperature. The subsequent modification is at 400 hours when the viscosity setpoint is changed. To accommodate this modification, the controllers act in a coordinated manner. This first part of the simulation is conducted to test the performance of the controllers separately. It can be observed that the CN-SIMC controllers impose a faster yet stabilized response similar to the SIMCs. Between 750 and 1200 hours, a disturbance of $+5L/h$ is added to both inputs. Thus, the controllers experience changes in both setpoints simultaneously at 1000 hours in the presence of disturbances. It can be verified that both controllers produce stable responses and behavior similar to what was expected, and they are capable of avoiding steady-state error. At 1300 hours, a new setpoint change is made in both variables for the system to return to the origin and proceed with the disturbance rejection test. At 1600 hours, a disturbance of $+5L/h$ is added to the solvent flow rate Qs and monomer flow rate Qm. The results indicate that the controllers' speed pattern is maintained, and both can mitigate the effects of these disturbances.

Additionally, Table 3 shows a series of performance indices used to compare the accumulated results in the experiment. The indices indicated as "MV" are calculated considering the error relative to the initial value of the series. These results indicate that the controllers are equivalent in performance and control effort.

Figure 4 presents two robustness tests. In the first one, on the left side of Figure 4, the controllers are tested against delays. In this test, the control actions were delayed by 15 sampling times. In the second test, on the right side of Figure 4, the aim is to seek the controller's gain margin. As proposed by Skogestad (2003), the SIMC controller has a gain margin (GM) of 3.14. In this test, a gain of $3 \cdot K_c$ was implemented for the initial setpoint changes for each controller at 10 hours and 300 hours. In Figure 4, it is possible to see that this value brings the NC-SIMC controller to the stability margin of the viscosity closed loop. At 600 hours, a gain of $1.5 \cdot K_c$ was used for both controllers, with a joint setpoint change. The results of the

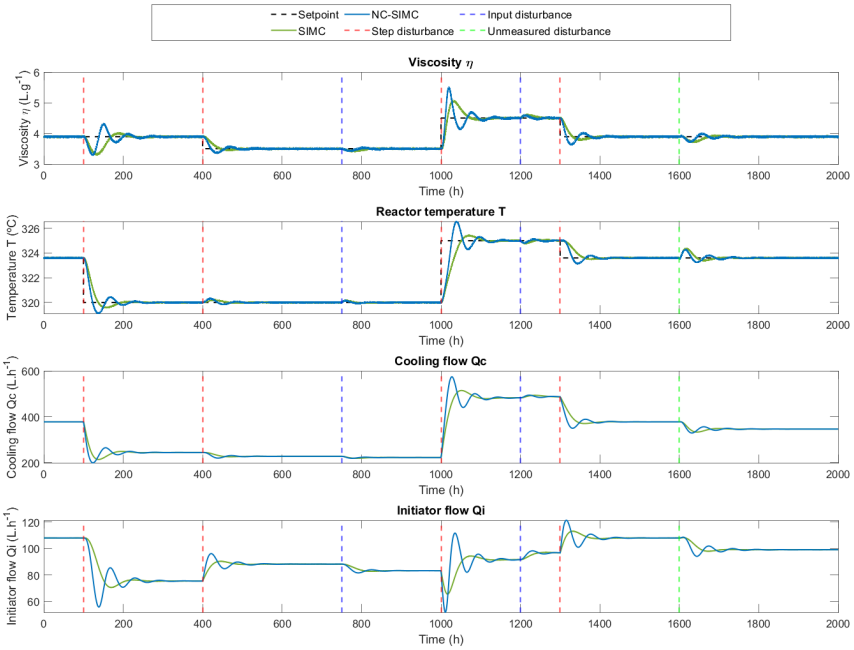

Fig. 3. Closed loop simulations of the NC-SIMC controller performance with setpoint change, noise and input disturbances. Sampling time 0.1 h.

Table 3. Performance index comparing the controllers on the case study of Figure 3.

Index	η		T	
	NC-SIMC	SIMC	NC-SIMC	SIMC
IAE	$1.04E+03$	$1.03E+03$	$3.12E+03$	$3.26E+03$
ISE	$3.42E+02$	$3.38E+02$	$5.36E+03$	$6.58E+03$
ITSE	$3.42E+01$	$3.38E+01$	$5.36E+02$	$6.58E+02$
ITAE	$1.04E+02$	$1.03E+02$	$3.12E+02$	$3.26E+02$
MAE	$5.21E-02$	$5.14E-02$	$1.56E-01$	$1.63E-01$
MSE	$1.71E-02$	$1.69E-02$	$2.68E-01$	$3.29E-01$
IAE-MV	$3.11E+05$	$3.06E+05$	$1.78E+06$	$1.77E+06$
ISE-MV	$7.44E+06$	$7.12E+06$	$2.35E+08$	$2.32E+08$
ITAE-MV	$3.11E+04$	$3.06E+04$	$1.78E+05$	$1.77E+05$
ITSE-MV	$7.44E+05$	$7.12E+05$	$2.35E+07$	$2.32E+07$
MAE-MV	$1.56E+01$	$1.53E+01$	$8.89E+01$	$8.85E+01$
MSE-MV	$3.72E+02$	$3.56E+02$	$1.17E+04$	$1.16E+04$

robustness tests show that the NC-SIMC controller tends to accelerate the closed-loop response. When compared with the responses from Figure 3, it is observed that this behavior is expected since the NC-SIMC controllers have a faster response than the SIMC. Similarly, Figure 2 shows that the NC-SIMC controllers were trained to achieve gains lower and higher than the value used as nominal in the SIMC. This indicates that the NC-SIMC controllers will modulate the speed of response based on the operating point.

4. CONCLUSIONS

This research introduces the Neuro-Controller Simple Internal Model Control (NC-SIMC), a novel hybrid neural network structure that integrates inductive bias and is trained following SIMC rules. The NC-SIMC employs an offline training methodology independent of closed-loop data, relying instead on tuning parameters derived directly from SIMC rules in an open-loop context. A key feature of this controller is the incorporation of an Inductive Bias layer, achieved through the use of a customized neuron. This neuron employs a Proportional-Integral (PI) activation function, enabling the network to generate control actions directly.

Our study's findings indicate that the NC-SIMC can deliver a stable response comparable to that achieved through traditional SIMC rule applications. This system's advantage is its ability to adapt to varying operating conditions, facilitating automatic and seamless adjustments in controller tuning. Opportunities exist to enhance this model's dynamic performance further and incorporate constraint handling more effectively. This could be achieved by integrating selectors directly into the inductive bias layer, thereby expanding the controller's capabilities in managing a broader range of operational scenarios.

ACKNOWLEDGEMENTS

The present work contributes to completion of a subproject at SUBPRO-Zero, a Research Center at the Norwegian University of Science and Technology. The authors would like to express their gratitude for the financial support received from SUBPRO-Zero, funded by the major industry partners, and NTNU.

REFERENCES

Alvarez, L.A. and Odloak, D. (2012). Optimization and control of a continuous polymerization reactor. *Brazilian Journal of Chemical Engineering*, 29(4), 807–820. doi:10.1590/S0104-66322012000400012. URL `https://doi.org/10.1590/S0104-66322012000400012`.

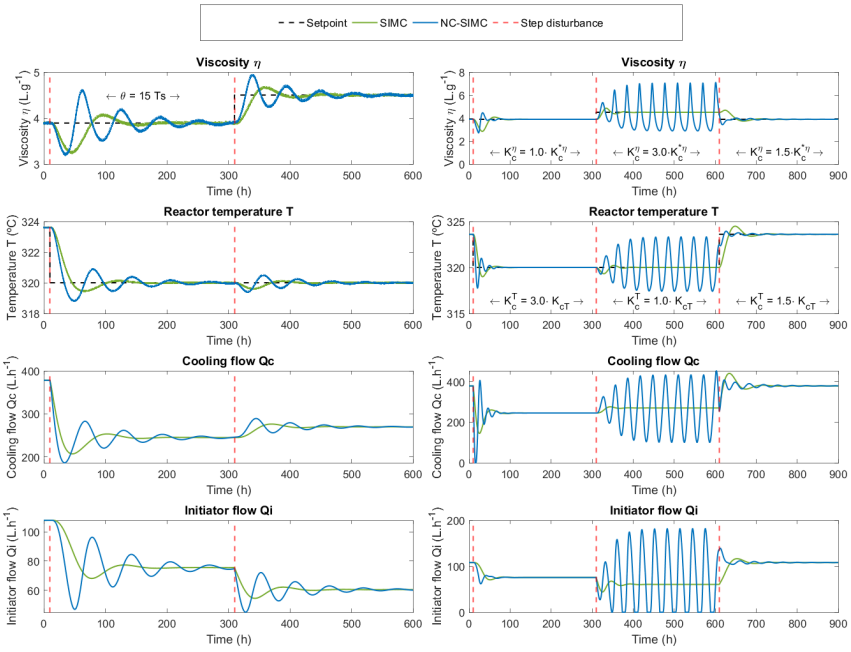

Fig. 4. Delay and margin gain robustness test.

Badr, A.Z. (1997). Neural network based adaptive pid controller. *IFAC Proceedings Volumes*, 30(6), 251–257. doi:https://doi.org/10.1016/S1474-6670(17)43373-8. IFAC Conference on Control of Industrial Systems "Control for the Future of the Youth", Belfort, France, 20-22 May.

de Moura, J.P., Neto, J.V.d.F., and Rego, P.H.M. (2020). A neuro-fuzzy model for online optimal tuning of pid controllers in industrial system applications to the mining sector. *IEEE Transactions on Fuzzy Systems*, 28(8), 1864–1877. doi:10.1109/tfuzz.2019.2923963. URL `http://dx.doi.org/10.1109/TFUZZ.2019.2923963`.

Garcia, C.E. and Morari, M. (1982). Internal model control. a unifying review and some new results. *Industrial & amp; Engineering Chemistry Process Design and Development*, 21(2), 308–323. doi:10.1021/i200017a016. URL `http://dx.doi.org/10.1021/i200017a016`.

Hernández-Alvarado, R., García-Valdovinos, L., Salgado-Jiménez, T., Gómez-Espinosa, A., and Fonseca-Navarro, F. (2016). Neural network-based self-tuning pid control for underwater vehicles. *Sensors*, 16(9), 1429. doi:10.3390/s16091429. URL `http://dx.doi.org/10.3390/s16091429`.

Hidalgo, P. and Brosilow, C. (1990). Nonlinear model predictive control of styrene polymerization at unstable operating points. *Computers & Chemical Engineering*, 14(4), 481–494. doi:https://doi.org/10.1016/0098-1354(90)87022-H.

Li, L., Jamieson, K., DeSalvo, G., Rostamizadeh, A., and Talwalkar, A. (2016). Hyperband: A novel bandit-based approach to hyperparameter optimization. *Journal of Machine Learning Research*, 18, 1–52. URL `http://arxiv.org/abs/1603.06560`.

Rivera, D.E., Morari, M., and Skogestad, S. (1986). Internal model control: Pid controller design. *Industrial & Engineering Chemistry Process Design and Development*, 25(1), 252–265. doi:10.1021/i200032a041.

Skogestad, S. (2003). Simple analytic rules for model reduction and pid controller tuning. *Journal of Process Control*, 13(4), 291–309. doi:https://doi.org/10.1016/S0959-1524(02)00062-8.

Xu, P. (2022). Neural network based self-tuning pid controller. In *2022 2nd International Conference on Algorithms, High Performance Computing and Artificial Intelligence (AHPCAI)*. IEEE. doi:10.1109/ahpcai57455.2022.10087411.

Ziegler, B.J.G. and Nichols, N.B. (1942). Optimum settings for automatic controllers. *Journal of Fluids Engineering*. URL `https://api.semanticscholar.org/CorpusID:41336178`.

Zribi, A., Chtourou, M., and Djemel, M. (2015). A new PID neural network controller design for nonlinear processes. *CoRR*, abs/1512.07529. URL `http://arxiv.org/abs/1512.07529`.